Anaphase Chromatid Motion: Involvement of Type II DNA Topoisomerases

Bertrand Duplantier,* Gérard Jannink,‡ and Jean-Louis Sikorav§
*Service de Physique Théorique, ‡Laboratoire Léon Brillouin, §Service de Biochimie et Génétique Moléculaire, Département de Biologie Cellulaire et Moléculaire, CEA/Saclay, 91191 Gif-sur-Yvette Cedex, France

ABSTRACT Sister chromatids are topologically intertwined at the onset of anaphase: their segregation during anaphase is known to require strand-passing activity by type II DNA topoisomerase. We propose that the removal of the intertwinings involves at the same time the traction of the mitotic spindle and the activity of topoisomerases. This implies that the velocity of the chromatids is compatible with the kinetic constraints imposed by the enzymatic reaction. We show that the greatest observed velocities (about 0.1 μm s^{-1}) are close to the theoretical upper bound compatible with both the diffusion rate (calculated here within a probabilistic model) and the measured reaction rate of the enzyme.

INTRODUCTION

In eukaryotic cells, the segregation of replicated chromatids to daughter cells occurs during anaphase: each chromatid pulled by the mitotic spindle moves apart with a roughly constant relative velocity V which ranges from 0.005 to 0.1 μm s^{-1} (these data have been reviewed by Mazia, 1961). This motion is known to be quite slow in comparison with other kinds of biological motions, which are often two orders of magnitude faster. We propose a tentative physical explanation for this slow motion.

It is now well established that the segregation of sister chromatids generally requires the removal of their intertwinings by type II DNA topoisomerases (topo II) (reviewed by Holm, 1994). The hypothesis put forward here is that the slow motion of the chromatids during anaphase results from a coupling between the enzymatic action of topo II and the traction of the spindle: the enzyme removes the intertwinings, while at the same time the spindle pulls apart the chromatids. This implies that the velocity of the chromatids is compatible with the kinetic constraints imposed by topo II.

The coupling mentioned above is crucial to the present work; for this reason, it is useful to discuss its mechanism, and why this mechanism is expected to be general. First, it is worth recalling that the idea that a coupling could exist between topo II activity and the spindle has been first proposed by Holm and co-workers, in the discussion of their work made in the budding yeast (Holm et al., 1985, 1989). According to these authors, the coupling exists because of the reversibility of the strand-passing reaction of topo II: in the metaphase chromosome, topo II catalyses a directionless tangling/untangling, until mitotic forces give direction to topo II. In other words, the coupling exists because the removal of the intertwinings *requires* at the same time the traction of the spindle and the enzymatic assitance of topo II. Although such a requirement can exist in the budding yeast, it is not necessarily expected to be a general one. Indeed, in some organisms where the mitotic spindle has been disrupted the separation of the chromatids is nevertheless ultimately observed, as if a "repulsion" appeared between the sister chromosomes (Mazia, 1961). We propose a slightly different mechanism for the coupling: the removal of the intertwinings *involves* (rather than *requires*) the simultaneous activity of the mitotic spindle and of topo II. Thus formulated, we believe that the mechanism is very general: 1) The observation that the sister chromatids can separate in the absence of spindle forces does not rule out the existence of the coupling in a standard anaphase. 2) The coupling has been observed by Bajer (1963) in the case of ring chromosomes, or dicentric chromosomes in a criss-cross configuration. In both cases the removal of the intertwinings during anaphase takes place in two steps. The standard fission, which generates the two daughter chromosomes, is followed by a second step during which the chromosomes, still interlocked, are pulled by the spindle and pass entirely through one another. It is clear that this second step requires the coupling that we propose. 3) The in vitro experiments of Shamu and Murray (1992) demonstrate that the chromatids remain catenated throughout metaphase and that decatenation takes place at the start of anaphase. These observations strongly suggest that the coupling is operating in their system.

We propose a model designed to describe the kinetic constraints associated with the simultaneous activity of the spindle and of topo II, as it appears in a standard anaphase. The main conclusion of the analysis made here is that the highest observed velocities are close to their theoretical upper bound compatible with the action of topoisomerases.

Received for publication 25 January 1995 and in final form 17 July 1995.

Address reprint requests to Dr. Bertrand Duplantier, Service de Physique Theorique, DSM - Bat. 774, CEA/Saclay, 91191 Gif-sur-Yvette Cedex, France. Tel.: 33 1 69 08 74 67; Fax: 33 1 69 08 81 20; E-mail: bertrand@amoco.saclay.cea.fr.

0006-3495/95/10/1596/10 $2.00

THE MODEL

Intertwining of the sister chromatids

In Fig. 1 we propose a schematic geometric description of a human metaphase chromosome composed of two inter-

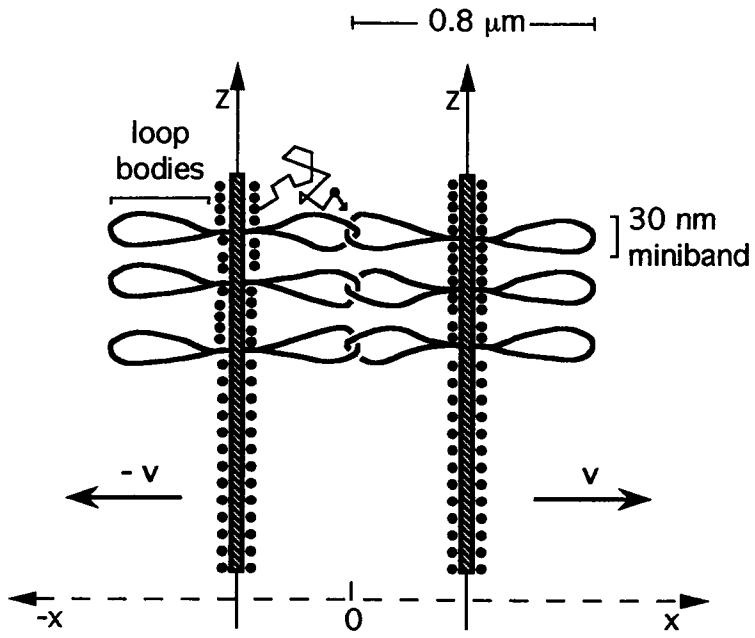

FIGURE 1 Schematic representation of the intertwining between the sister chromatids at the onset of anaphase. The chromatids are displayed with a radial loop organization. DNA loops stem from the metaphase scaffold (striped) which is shown here located at the center of the chromatids. The entanglements between the chromatids occur at peripheral locations. Topo II dimers (shown as black dots) are located initially at the center of the chromatids. They must diffuse via Brownian motion (broken arrow) over a length $L \approx 0.4$ μm to reach the entanglements. This description is only valid for the *R* bands of the chromatids; for other regions of the chromosome, the scaffold probably assumes a more complex coiling (Saitoh and Laemmli, 1994), and the distance between the scaffold and the entanglements would only be a fraction of *L*.

twined linear replicated chromatids. Each sister chromatid has a cylindrical structure. The two cylinders partially overlap, and the intertwinings between the sister chromatids are naturally located in the overlap region. Within each chromatid, the DNA molecule is folded according to the radial loop model proposed by Laemmli and co-workers (Saitoh and Laemmli, 1994). In this model, the DNA molecule is folded into loops of about 60 kb each. We further assume here that the chromatids are organized in densely packed minibands (shown unstacked in Fig. 1), each of which contains about 18 radial loops of 60 kb (Pienta and Coffey, 1984). Using this information, we estimate the amount of interlocks between the two sister chromatids in the following manner.

1) We follow the assumption that the interlocks originate from the termination of the replication process, at the merging of converging replication forks; in this process 10 to 30 interlocks would be created at each termination region associated with a given replicon (Sundin and Varshavsky, 1981; Wang, 1991). For an average replicon size of about 40 kb, the resulting interlock density ranges from ¼ to ¾ interlock per kilobase.

2) Many of the interlocks between the sister chromatids appear to be removed during chromosome condensation, as implied by the overall structure of the metaphase chromosome, with the two sister chromatids lying side by side. The interlocks must be removed by the topoisomerases, but because this enzyme acts in a reversible manner, there must exist an energetic drive providing the direction of the reaction. The mechanism is unknown; it could involve the intervention of a DNA helicase (Watt et al., 1995). It is also possible that the 10 to 30 interlocks between the sister chromatids locally distort the helical geometry of the DNA molecules and that this distortion provides the directional energetic drive for the removal of the interlocks by topo II (Wasserman et al., 1986; Permana et al., 1994). In such a manner, the number of interlocks could be reduced from 10–30 down to one; when a single interlock remains the directional drive is missing and a topo II alone becomes inefficient. This should be the situation at the onset of anaphase, before the traction exerted by the spindle.

Here, we propose that of the 18 radial loops of a miniband, about one-third overlap and are intertwined with the loops of a sister chromatid. The number of interlocks between the sister chromatids per unit length is therefore 300 μm^{-1} (one remaining interlock per 40 kb; 6×60 kb = 360 kb of intertwined DNA per 30-nm-thick miniband).

Removal of the interlocks

At the onset of anaphase ($t = 0$) the metaphase chromosome undergoes a longitudinal fission, which generates the two daughter chromosomes. The sister chromatids, pulled by the mitotic spindle, move apart with a given relative velocity $V = 2v$, where v is the absolute velocity. Entanglements (stress points) appear between the interlocked loops of the chromatids. Topo II, which are known to bind preferentially to cross-overs of two DNA double helices (Zechiedrich and Osheroff, 1990), bind to these entanglements and pass the two DNA segments through one another. The model can be described by several characteristic times. The first time, $\tau_{contact}$, is the time during which the two chains that constitute an entanglement remain in contact. The minimum contact time corresponds to the idealized situation where the two chains pass through one another without any deformation, and this minimum is $\tau_{contact} = d/v$, where d is the diameter of a DNA double helix. However, $\tau_{contact}$ could be greatly increased if deformations of the sister chromatids occur during anaphase (such deformations are indeed ob-

served in the segregation of ring or dicentric chromosomes mentioned above; Bajer, 1963). For linear chromatids such as those considered here, we actually know that the fission can take place without major deformation, through a rigid separation of the chromatids occuring synchronously all along the length of the chromosome (Bajer and Molé-Bajer, 1972). Such observations rule out possible deformations of the chromatids due to persisting, lagging entanglements. Furthermore, once anaphase has begun, the addition of inhibitors of topo II has no effect (Downes et al., 1991; note, however, that the time at which the inhibitors were added was not precisely defined in that work). Thus the absence of deformation of the sister chromatids implies that they cease to be intertwined before they have migrated a distance L equal to their own radius, $L \approx 0.4$ μm (a rough measure of the overlap interval). This defines a second characteristic time, the fission time $\tau_{\text{fission}} \approx L/2v$, which gives an upper bound to the contact time: $\tau_{\text{contact}} < \tau_{\text{fission}}$. For the maximum observed velocities, $v = V/2 \approx 0.05$ μm s^{-1}, and $\tau_{\text{fission}} \approx 4$ s.

The time τ_{fission} must encompass the overall time τ_{overall} required for the action of the enzyme, which in turn involves two characteristic times.

The first, τ_{cross}, is the average time required locally by one topo II to catalyze a single strand-passage reaction at a particular entanglement. It is equal to the reciprocal of the turnover number of the enzyme, as $\tau_{\text{cross}} = k^{-1}{}_{\text{cat}}$ ($k^{-1}{}_{\text{cat}}$ is also known as the transit time; Fersht, 1985). We shall use here the values determined experimentally from the relaxation of supercoiled DNA, $k^{-1}{}_{\text{cat}} \approx 1$ s (Osheroff et al., 1983; Lindsley and Wang, 1993). With this estimate, τ_{cross} is close to τ_{fission} (for $v = 0.05$ μm s^{-1}). If a single topo II had to remove more than one interlock, the time needed would be greater than τ_{cross}. However, this situation is unlikely, because the number of available topo II exceeds interlocks to be removed (see below).

The second time is the average time required for topo II to diffuse to the entanglement sites. The existence of a diffusive process is supported by the following arguments.

1) The diffusion of topo II during mitosis has been observed (Swedlow et al., 1993). The enzyme present in the early prophase chromosome is lost in the surrounding cytoplasm in two stages, 60% during metaphase and 10% during anaphase. For our purpose, we agree with Swedlow et al. (1993) that topo II diffuse to the (entanglement) sites where they are required.

2) As shown in Fig. 1, the entanglements occur at the periphery of the sister chromatids. Furthermore, termination of DNA replication (where the entanglements are located) takes place at random sequences (Zhu et al., 1992; Hyrien and Mechali, 1993). By contrast, at the onset of anaphase, topo II are likely to be located at particular DNA sequences, known as the scaffold-associated regions (SAR). Following the radial loop model, the SAR (and hence topo II) are located at the bases of the loops, at the center of the chromatids (see Fig. 1).

Let us now estimate the amount of topo II available for the removal of the interlocks.

1) Each chromatid contains 1 topo II dimer per 40 kb (Gasser et al., 1986). This yields a linear topo II density of 900 dimers μm^{-1} (assuming 18 loops of 60 kb per 30-nm-thick miniband).

2) We identify the fraction of topo II involved in the removal of the interlocks with the fraction observed to diffuse from the chromosome during anaphase, i.e., 25% of the chromosomal topo II remaining at the end of metaphase (Swedlow et al., 1993). Taking into account the contributions of the two chromatids, the linear density of active topo II is therefore $n_0 = 450$ dimers μm^{-1}.

Topo II diffusion to the entanglements

We propose now a geometrical model that describes the Brownian probability $P_1(t)$ that a given entanglement is reached by time t by any topo II ($t = 0$ being the onset of anaphase). It is based on the following assumptions: 1) At $t = 0$, the topo II located close to the scaffold leave for entanglements localized at about a distance L. 2) The diffusion medium is dragged away at constant speed v or $-v$. 3) The enzyme diffuses with a diffusion constant D.

The probability for a Brownian particle starting from the origin O to have reached by time t the interior of a ball of radius ε centered at a distance r from O, is given asymptotically for small ε by (Le Gall, 1986)

$$\mathcal{P}(r, t) = 4\pi D\varepsilon \int_0^t \frac{dt'}{(4\pi Dt')^{3/2}} \exp(-r^2/4Dt'). \quad (1)$$

where D is the diffusion constant of the particle.

A given Brownian topo II located at a transverse distance $x = \pm L$ starts at altitude z above its target entanglement (see Fig. 1). Furthermore, the topoisomerase is moving away with velocity $\pm v$ and we thus substitute to r^2 in Eq. 1

$$r^2(z, t') \equiv (L + vt')^2 + z^2. \quad (2)$$

The probability that this entanglement is removed by time t by a topo II is given by

$$\mathcal{P}(z, t) = 4\pi D\varepsilon \int_0^t \frac{dt'}{(4\pi Dt')^{3/2}} \exp[-r^2(z, t')/4Dt']. \quad (3)$$

Let us suppose that there are N topo II, $i = 1, \cdots, N$, located at altitudes z_i. The total probability $P_1(t)$ that the entanglement is removed by time t by any of these topo II is given by the equation

$$1 - P_1(t) = \prod_{i=1}^{N} [1 - \mathcal{P}(z_i, t)]. \quad (4)$$

We replace the discrete set of topo II located along the scaffold by a continuum model characterized by the uniform

linear density n_0 along the z axis. Taking the large N limit in Eq. 4 we obtain

$$P_1(t) = 1 - \exp \int_{-L'}^{L'} n_0 \, dz \ln[1 - \mathcal{P}(z, t)]. \quad (5)$$

In Eq. 5, the introduction of an integration height $2L'$ corresponds roughly to the existence of R-band structures in the chromatids (Saitoh and Laemmli, 1994). This will be discussed in more detail below.

Numerical calculations of $P_1(t)$ require, in addition to the value of n_0 estimated above, knowledge of the biological parameters ε, D, and L'.

1) Considering the entanglement as localized, we take ε to be the estimated radius of a topo II, $\varepsilon \approx 6.4\ 10^{-3}\ \mu$m (Krueger et al., 1990).

2) The model also requires the knowledge of the diffusion constant D of topo II. The diffusion coefficient D_0 of topo II in dilute solutions has been determined by dynamic light scattering for the prokaryotic topo II, $D_0 = 34\ \mu\text{m}^2\ \text{s}^{-1}$ (Krueger et al., 1990). We expect D to be much smaller than D_0. The two cases must be distinguished.

a) The enzyme diffuses within the chromatid medium. According to the model proposed by Pienta and Coffey (1984), about 16% of the volume of the metaphase chromosome is occupied by the nucleosomal fibers. From experiments on the diffusion of tracer proteins in the presence of polymers (Zimmermann and Minton, 1993), it is reasonable to expect D to be smaller than D_0 by two orders of magnitude. In reality, the 16% of the volume fraction could be much greater (indeed, in cryo-electron microscopy the metaphase chromatid resembles a "sea of nucleosomes"; McDowall et al., 1986). This would lead to even lower values of D.

b) The enzyme diffuses in the surrounding cytoplasm. The viscosity of the cytoplasm during anaphase is about 3×10^2 that of water (Taylor, 1965; Alexander and Rieder, 1991). In that case we also expect D to be smaller than D_0 by two orders of magnitude.

We therefore take $D = 0.34\ \mu\text{m}^2\ \text{s}^{-1}$, knowing that this figure is likely to overestimate the diffusion coefficient.

3) The sister chromatids are thought to possess a complex structure, made of bands Q and bands R (Saitoh and Laemmli, 1994). The model shown in Fig. 1 is strictly valid for R bands; outside the R bands (in the Q bands) the scaffold probably assumes a more complex coiling (Rattner and Lin, 1985; Saitoh and Laemmli, 1994). In the Q bands, there should be fewer intertwinings, more topo II, and a reduced distance between the scaffold and the intertwinings. For these three reasons, we believe that the kinetic constraint that we analyze here is much less severe outside the R bands. We could take, a priori, as an estimate for L' the height of an R band. However, this would greatly underestimate the intervention of the topoisomerases of the Q bands, which can also participate in the removal of the intertwinings of the R bands. In the absence of any information on this question, we have extended the height $L' = \alpha L$ to large values of α, taking typically $\alpha = 10$. Because of the exponential decay of $P(z, t)$ with variable z, the convergence to $\alpha \to \infty$ is fast, and the results obtained in this manner should be robust.

It is physically instructive to rewrite the (dimensionless) probability $P_1(t)$ in terms of fully dimensionless variables. By inspection of Eqs. 1, 2, and 3 it appears that it is useful to introduce the time-like variable

$$x = \frac{v^2 t}{4D} \quad (6)$$

and its associated integration variable $\theta = v^2 t'/4D$, together with the second dimensionless variable

$$y = \frac{Lv}{2D}, \quad (7)$$

so that $\mathcal{P}(z, t)$ in (3) now reads explicitly

$$\mathcal{P}(z, t) = \frac{1}{2\sqrt{\pi}} \frac{\varepsilon}{L} y \int_0^x \frac{d\theta}{\theta^{3/2}} \exp\left\{-\theta - y - \frac{y^2}{4\theta}\left[1 + \left(\frac{z}{L}\right)^2\right]\right\}. \quad (8)$$

The height z is measured in units of $L' = \alpha L$, so, using $u = z/L$, we arrive for $P_1(t)$ (Eq. 5) at

$$P_1(t) \equiv P(x, y) = 1 - \exp\left\{2n_0 L \int_0^\alpha du \ln(1 - \mathcal{P}[u, x, y])\right\}. \quad (9)$$

with

$$\mathcal{P}[u, x, y] = \frac{1}{2\sqrt{\pi}} \frac{\varepsilon}{L} y e^{-y} \int_0^x \frac{d\theta}{\theta^{3/2}} \exp\left[-\theta - \frac{y^2}{4\theta}(1 + u^2)\right]. \quad (10)$$

Thus $P_1(t)$ really appears as a function $P(x, y)$ of the dimensionless variables $x = v^2 t/4D$, $y = Lv/2D$, $n_0 L$, ε/L, and $\alpha = L'/L$. We now focus on the dependence on the two biologically relevant ones, namely x and y, both being associated with the segregation speed v, and the last three parameters can be considered as fixed by construction of the model. In our case, we have proposed above

$$n_0 \simeq 450\ \mu\text{m}^{-1}, \quad L \simeq 0.4\ \mu\text{m}, \quad \varepsilon \simeq 6.4\ 10^{-3}\ \mu\text{m},$$

thus

$$n_0 L \simeq 180, \quad \frac{\varepsilon}{L} \simeq 1.6\ 10^{-2}, \quad \text{and} \quad \alpha = \frac{L'}{L} \simeq 10. \quad (11)$$

Because of the small value of ε/L, the partial probability $P[u, x, y]$ (Eq. 10) will take only small values. Therefore, a good and simpler form can be obtained by retaining in Eq. 9 only the first term of the expansion

$$\ln(1 - \mathcal{P}[u, x, y]) = -\mathcal{P}[u, x, y] + \cdots, \quad (12)$$

so that

$$P_1(t) \equiv P(x, y) \simeq \tilde{P}_1(t) \equiv \tilde{P}(x, y) \equiv 1 - \exp\left\{-2n_0 L \int_0^\alpha du\, \mathcal{P}[u, x, y]\right\}. \quad (13)$$

In this formula the integral over u is easily performed with the help of Eq. 10, leading to

$$\tilde{P}_1(t) \equiv \tilde{P}(x, y) \quad (14)$$

$$= 1 - \exp\left\{-n_0 \varepsilon e^{-y} \int_0^x \frac{d\theta}{\theta} \exp\left(-\theta - \frac{y^2}{4\theta}\right) \mathrm{Erf}\left(\frac{y\alpha}{2\sqrt{\theta}}\right)\right\},$$

where Erf denotes the standard error function

$$\mathrm{Erf}(z) = \frac{2}{\sqrt{\pi}} \int_0^z e^{-t^2}\, dt \quad (15)$$

The numerical calculation of the double integral in (9) or of the simple integral in (14) shows that indeed these two formulae are equal within a 10^{-3} error bar, leading to *indistinguishable* curves as functions of t or y. For the large value $\alpha = 10$, one can even take in the whole range $\mathrm{Erf}(y\alpha/2\sqrt{\theta}) \simeq 1$, leading to the even simpler formula

$$\hat{P}_1(t) \equiv \hat{P}(x, y) = 1 - \exp\left\{-n_0 \varepsilon e^{-y} \int_0^x \frac{d\theta}{\theta} e^{-\theta - y^2/4\theta}\right\}, \quad (16)$$

which again leads to curves indistinguishable from P (9) or $\tilde{P}$ (14). Therefore Eq. 16 is obviously sufficient for our purpose, considering the numerous hypotheses proposed for defining our model.

In Fig. 2 we have drawn the curves $P_1(t)$ (or $\tilde{P}_1(t)$, or $\hat{P}_1(t)$) as functions of time t, for several plausible sets of values of v and D. The case (a) is the reference one: $v = 0.05\ \mu\mathrm{m\ s^{-1}}$, and $D = 0.34\ \mu\mathrm{m^2\ s^{-1}}$. The maximum allowed time, $t = 4$ s, corresponds to the associated fission time τ_{fission}. Cases (b), (c), (d), and (e) are derived from the reference case (a) by the following respective substitutions: $v \rightarrow 5v$ (case (b)); $v \rightarrow 10v$ (case (c)); $D \rightarrow D/5$ (case (d)); and $D \rightarrow D/10$ (case (e)). The probability $P_1(t)$ reaches a value extremely close to 1 in less than $\tau_{\mathrm{fission}} = 4$ s for cases (a) and (b). In contrast, this is not true for cases (c), (d), and (e). The main conclusion is already apparent: the constraint associated with the diffusion process is stringent. Multiplying the velocity v by one order of magnitude (case (c)) or dividing the diffusion constant by a factor 5 (case (d)) renders the diffusion process inefficient.

This is even clearer when one recalls that $P_1(t)$ is the probability that a *single* given entanglement is removed by any of the diffusing topo II before time t, while *all* the entanglements of a given R band should be removed in the same period. Because there are about 1000 R bands in human metaphase chromosomes, a typical R band should

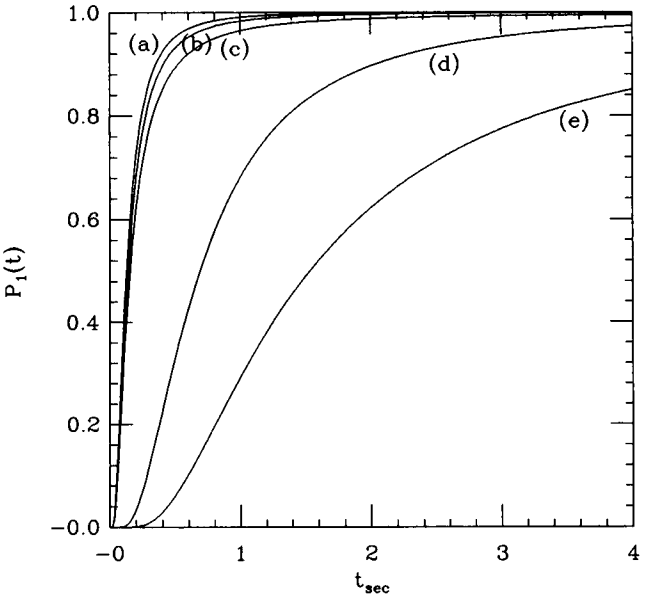

FIGURE 2 Probability $P_1(t)$ that a given entanglement is reached by time t by any topo II. (*a*) $D = D_0/100 = 0.34\ \mu\mathrm{m^2\ s^{-1}}$, $L = 0.4\ \mu$m, $v = 0.05\ \mu\mathrm{m\ s^{-1}}$; and cases derived from (*a*) by substitution: (*b*) 5*v*; (*c*) 10*v*; (*d*) *D*/5; (*e*) *D*/10.

contain about 100 entanglements. (The human genome contains 3.3×10^6 kb, and there should be approximately one entanglement per 40 kb.) Assuming that the different available topo II act independently, the probability of removing all the entanglements of a typical R band is taken equal to $[P_1(t)]^{100}$. The corresponding curves are drawn in Fig. 3. They allow us to discriminate between cases (a) and (b): multiplying the velocity by 5 (case (b)) already greatly

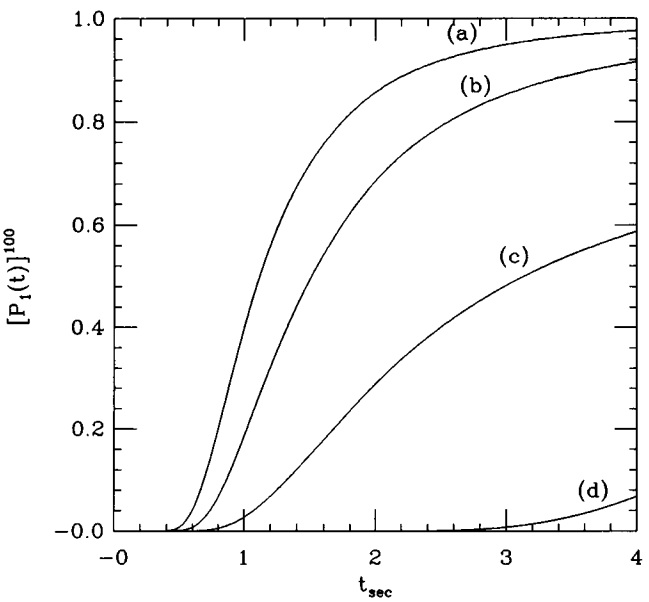

FIGURE 3 Probability $[P_1(t)]^{100}$ of removing all the entanglements of an R band by time t corresponding to the same five cases as in Fig. 2.

reduces the efficiency of the process. Because the standard case (a) has been selected from a maximal observed value for v, we can assume that in reality anaphase does take place under conditions imposed by the efficiency constraints described by the model.

Efficiency of the diffusion process as a function of the velocity

We have seen in Eqs. 9 and 10 that the probability $P_1(t)$ is a function of the two dimensionless variables $x = v^2t/4D$ and $y = Lv/2D$ (Eqs. 6 and 7). Here we study the efficiency of the diffusion process at a given time as a function of the segregation speed v. More precisely, we consider times t of the order of the fission time $\tau_{\text{fission}} = L/2v$. Let us thus set

$$t = 4\beta\tau_{\text{fission}}, \tag{17}$$

where β is an arbitrary proportionality constant. This is equivalent to the simple formula

$$x = \beta y, \tag{18}$$

such that now

$$P_1(t = 4\beta\tau_{\text{fission}}) \equiv P(x = \beta y, y) \tag{19}$$

Notice that the variable y itself appears as a proportionality constant between a typical diffusion time $\tau_{\text{diff.}} = L^2/2D$ and $\tau_{\text{fission}} = L/2v$:

$$\tau_{\text{diff.}} = 2y\tau_{\text{fission}},$$

and is known as the Sherwood number (Purcell, 1977). It appears typically in phenomena involving a competition between diffusion and drag.

In Fig. 4, we have drawn the curves $P(\beta y,y)$ as a function of y, keeping as above the values (11) for the other parameters $n_0L,\varepsilon/L$, and α. The case (a) $\beta \to \infty$, corresponds to the large time value $P_1(t \to \infty)$, explicitly calculated in Appendix A (for very large α). The next case (b) corresponds to the value $\beta = 1/4$, thus $t = \tau_{\text{fission}}$, whereas cases (c) and (d) correspond to shorter times: $\beta = 1/8$, $t = 1/2\tau_{\text{fission}}$ and $\beta = 1/40$, $t = 1/10\tau_{\text{fission}}$. The large time limit $\beta \to \infty$ is the envelope of the others and has the following features.

At small values of y, $P(\infty, y)$ reaches the maximal value 1 algebraically fast and with a zero slope, according to the law (Appendix A, for $\alpha = \infty$)

$$P(\infty, y) \underset{y\to 0}{\cong} 1 - cy^{2n_0\varepsilon} \tag{20}$$

where (see Eq. 11) $2n_0\varepsilon \simeq 5$–6.

At large values of y, $P(\infty, y)$ decreases to zero exponentially fast in terms of the Sherwood number y, as established in Appendix A:

$$P(\infty, y) \underset{y\to\infty}{\simeq} 2n_0\varepsilon\, e^{-2y} \sqrt{\frac{\pi}{2y}}. \tag{21}$$

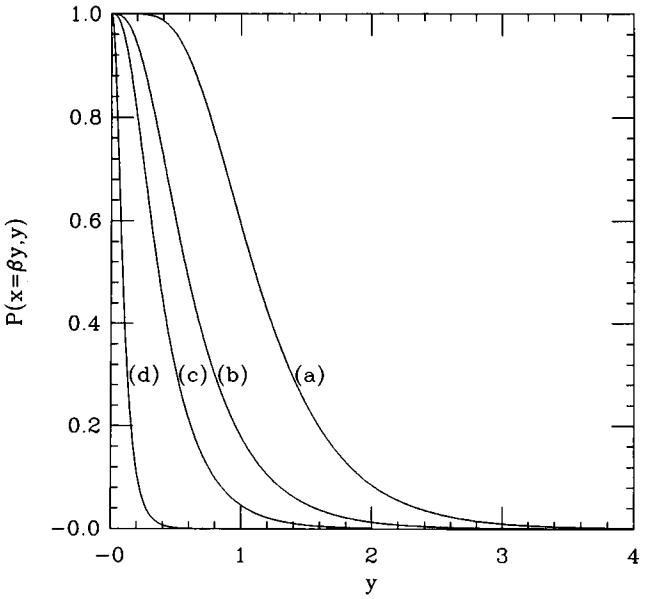

FIGURE 4 Single entanglement removal probability $P(x = \beta y, y)$ as a function of the parameter $y = Lv/2D$, drawn for $\beta = \infty$ (*a*); $\beta = 1/4$ (*b*); $\beta = 1/8$ (*c*); $\beta = 1/40$ (*d*). This corresponds to fixed time evaluation at $t = 4\beta\tau_{\text{fission}}$.

For finite values of the diffusion time t, i.e. β, the curves $P(\beta y, y)$ have features similar to those of $P(\infty, y)$ (Fig. 4). At zero Sherwood number y, they all start from the upper limit 1: $P(\beta y, y)\,|_{y=0} = 1$.

This is actually due to the choice of a large effective height $L' = \alpha$L, $\alpha = 10$ for R bands. Indeed, a more refined study (Appendix B) shows that as a function of α

$$P(\beta y, y, \alpha)\,|_{y=0} \underset{\alpha\to\infty}{\simeq} 1 - (2\alpha)^{-2n_0\varepsilon}, \tag{22}$$

which explains why for $2n_0\varepsilon \simeq 5$–6, the numerical case of Fig. 4 $\alpha = 10$ is already indistinguishable from that of $\alpha \to \infty$.

At large values of y, all curves $P(\beta y, y)$ decrease exponentially fast with y. This is immediately seen in Fig. 4, and follows mathematically from the obvious inequality

$$P(\beta y, y) < P(\infty, y) \tag{23}$$

and from the asymptotic law (21).

This means that the existence of a diffusion process leads to a stringent condition for v which must adjust to D. As discussed already, the curves in Fig. 4 describe the probability of removing a single entanglement. The efficiency curves corresponding to the removal of all the entanglements of an R band (taken equal to $[P(\beta y, y)]^{100}$) are drawn in Fig. 5 for the same four values of parameter β. They display the same characteristic features discussed above, but they decrease to zero for much smaller values of y.

In the standard case considered here (case (a) of Fig. 2), the values of the parameters are $L = 0.4$ μm, $v = 0.05$ μm s^{-1} and $D = 0.34$ μm^2 s^{-1}, leading to a standard value of y: $y_{\text{st}} = 0.029$. In Table 1 we give the corresponding values

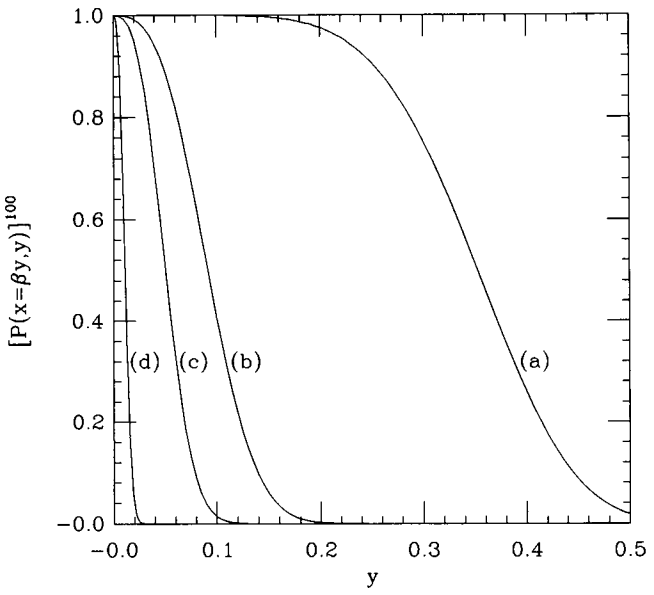

FIGURE 5 R band entanglements removal probability $[P(x = \beta y, y)]^{100}$ corresponding to the same four cases as in Fig. 4.

of $P(\beta y, y)$ and $[P(\beta y, y)]^{100}$ at $y = y_{st}$ associated with the four values of β considered in Fig. 5. It can be seen that the diffusion process is inefficient for the small values of the parameter β (curves (d) and (c)): one has to wait for a time of the order $\tau_{fission}$ to reach a probability close to 1 (curve (b)).

An inspection of curve (a) in Fig. 5 corresponding to the infinite time $\beta \rightarrow \infty$ allows us to estimate a maximal value of y compatible with the diffusion process. Indeed, at $y^* \approx 0.1$, $[P(\infty, y)]^{100}$ falls from the value 1. The corresponding velocity v^* is equal to $v^* \approx 0.16\ \mu m\ s^{-1}$, only three times higher than the greatest observed velocity $v = 0.05\ \mu m\ s^{-1}$.

DISCUSSION

We have examined the proposal that in a standard anaphase, the removal of the last intertwinings between the sister chromatids is performed by the topo II, while at the same time the mitotic spindle pulls the chromatids apart. The main conclusion is, that to allow a smooth and biological safe segregation, the velocity v is limited by the inequality

$$\tau_{overall} \lesssim \tau_{fission} = L/v,$$

or, equivalently,

$$v \lesssim L(\tau_{overall})^{-1} \qquad (24)$$

where $\tau_{overall}$ is the time required for the action of topo II. The time overall is the sum of $\tau_{cross} = k^{-1}{}_{cat}$ and τ_{diff}, the average time required for topo II to diffuse to the entanglement sites. To study this diffusion process, we have proposed a probabilistic model designed to capture the search

TABLE 1 Values of the efficiency function for an R band $[P(\beta y_{st}, y_{st})]^{100}$, for the reference parameter $y_{st} = 0.029$ corresponding to case (a) of Fig. 2 and for the four values of β of Figs. 4 and 5

β	∞	1/4	1/8	1/40
$P(\beta y_{st}, y_{st})$	1.0000	0.9998	0.9985	0.9241
$[P(\beta y_{st}, y_{st})]^{100}$	0.9999	0.9762	0.8583	$0.37\ 10^{-3}$

of topological constraints by diffusing enzymes. In this model, the efficiency of the diffusion process is described by the probability that all the entanglements of an R band have been reached by time t by diffusing topo II. This probability decreases with increasing values of v: the maximal velocity v^* compatible with an efficient process is equal to $v^* \approx 0.16\ \mu m\ s^{-1}$, very close to the greatest observed velocity $v = 0.05\ \mu m\ s^{-1}$. Under the conditions of a standard anaphase, we find that this probability reaches a value close to 1 in a time (the diffusion time) of the order of the fission time. Thus inequality (24) appears very stringent. We note that the time τ_{diff} is not strictly required; we have considered a value of $[P_1(t)]^{100}$ greater than 0.95 as sufficiently close to 1, but this is rather arbitrary.

The coupling that takes place during the fission process between the enzymatic activity of topo II and the traction of the spindle leads to kinetic constraints that are expressed in terms of consistent relations between v, $k^{-1}{}_{cat}$, and D. Although the fission occupies a small fraction of the duration of anaphase, these constraints apparently dictate the uniform velocity of the chromosomes, even after the removal of the interlocks. The kinematic reasoning developed here can be extended to an analysis of the dynamics of the fission process (i.e., involving the force exerted by the spindle; see the review of Nicklas, 1988; and manuscript in preparation).

Validity of the model

The model discussed here for a standard anaphase rests on several assumptions. In particular, to analyze the diffusion process, we have used a very simple geometrical model in which the chromatids are described as partially overlapping cylinders, and where the topo II are initially located at the center of the chromatids. The enzymes are also supposed to be dragged away with a constant velocity; this is a non-draining hypothesis which remains to be proved. On the other hand, the fission process occurs in various organisms under conditions that may significantly differ from those of a standard anaphase. Both these assumptions and these variations can limit the validity of the model, as discussed now.

1) The assumption that the fission requires the assistance of topo II is not valid for short enough linear chromosomes; Spell and Holm (1994) have shown that in the yeast *S. cerevisiae*, small chromosomes (380 kb or smaller) can

segregate in the absence of enzyme. The model does not apply to these small chromosomes. For larger chromosomes, one can actually show that the fission requires the action of topo II; this will be discussed elsewhere.

2) We have studied the removal of interlocks present at the periphery of cylindrical sister chromatids. In a number of cases, however, the structure of the metaphase chromosome is more intricate. We have mentioned already the case of ring chromosomes, where one chromosome appears to pass entirely through another one (Bajer, 1963). Also, the sister chromatids can be plectonemically coiled (Sparrow et al., 1941), again leading to more complex problems during segregation.

3) The diffusion process would be accelerated if the topo II were not initially located at the center of the chromatids. This could happen even in the case of a scaffold-associated distribution outside the R bands as noted above, or for a bulk rather than scaffold-associated distribution of topo II in the chromatid. Such a distribution has been favored by Swedlow et al. (1993). The existence of two distinct types topo II in mammalian cells is also in favor of a bulk distribution of topo II in these cells: Drake et al. (1989) have proposed that one of the two types is associated with the scaffold, whereas the other is more diffuse in the cytoplasm. In this respect we observe that the model proposed here is a "coconut tree model": at $t = 0$, when the chromatids are set in motion, the topo II are supposed to leave the scaffold like coconuts falling from a shaken tree. In a plausible alternative, topo II could already be diffusing before anaphase onset. The mathematics of diffusion process involving a more homogeneous distribution of topo II in the cylinders could be worked out. We expect, however, that the constraints are similar to those described here.

Enzymatic perfection during anaphase

It is noteworthy that $k_{cat} \approx 1\ s^{-1}$ for topo II. This figure seems large in view of the complex reaction performed by the enzyme (a transient double-strand break, followed by the passage of the second DNA segment through the break, and terminated by the resealing of the break). In comparison, the k_{cat} of restriction enzymes, which perform solely cleavage reactions, is usually two orders of magnitude smaller (Bennet and Halford, 1989). The difference between the two rate constants is likely to reflect an adaptation to a particular biological role. For restriction enzymes an erroneous cleavage of DNA can be lethal; accuracy rather than speed should be advantageous. In the case of topo II, the strand-passage reaction defines a relative velocity $V_{topo} = 2d \times k_{cat}$ (where $d = 2$ nm is the thickness of a double helix), which cannot be much smaller than v, as explained in this work. Thus, the adaptation to this particular task requires a high k_{cat} for topo II. It is worth mentioning here that the value of $k_{cat} \simeq 1\ s^{-1}$ could underestimate the true k_{cat}; preliminary results of Grosse and Langowski obtained from quench-flow studies (quoted in Schomburg and Grosse, 1986) suggest that k_{cat} could be greater than $30\ s^{-1}$. It will be of interest to confirm these results. The low value of the velocity v (in comparison with other types of biological motion) is in fact close to the highest value compatible with the action of topo II. "Enzymatic perfection" occurs when the turnover number of the enzymatic reaction equals the diffusion velocity of the substrate (Albery and Knowles, 1976). Here $k^{-1}{}_{cat} = \tau_{cross} \approx \tau_{diff}$, and both times are close to their upper limit $\tau_{fission} \approx L/2v$. Sister chromatid segregation in the presence of topoisomerase may thus be viewed as a particular example of enzymatic perfection.

APPENDIX A

Large t limit of $P_1(t)$

We are interested in the limit probability $P_1(t \to \infty)$. It can be obtained from Eqs. 6, 9, and 10 in the limit $x \to \infty$. The integral (10) $\mathcal{P}[u, x \to \infty, y]$ can be evaluated with the help of (Gradshteyn and Ryzhik, 1980)

$$\int_0^\infty \exp(-ax'^2 - b/x'^2)\, dx' = \frac{1}{2}\sqrt{\frac{\pi}{a}}\exp(-2\sqrt{ab})$$

to be

$$\mathcal{P}[u, x \to \infty, y] = \frac{\varepsilon}{L} e^{-y}(1+u^2)^{-1/2}\exp[-y(1+u^2)^{1/2}]. \tag{A.1}$$

For α large this leads to an explicit asymptotic one-entanglement probability

$$P_1(t \to \infty) = 1 - \exp[2n_0 L F(y)] \tag{A.2}$$

$$F(y) = \int_0^\infty du \ln\left[1 - \frac{\varepsilon}{L} e^{-y} \frac{1}{\sqrt{1+u^2}} \exp(-y\sqrt{1+u^2})\right].$$

We expand in powers of the small parameter

$$a = \frac{\varepsilon}{L} e^{-y} \tag{A.3}$$

and perform the change of integration variable $u = \text{sh}\, u'$, $du = \text{ch}\, u'\, du'$, so that

$$F(y) = -\sum_{n>0} a^{n+1} I_n(y) \tag{A.4}$$

$$I_n(y) = \frac{1}{n+1}\int_0^\infty du'(\text{ch}\, u')^{-n} e^{-(n+1)y\,\text{ch}\,u'}. \tag{A.5}$$

These integrals $I_n(y)$ satisfy the recursion relations

$$\frac{d^n}{dy^n} I_n(y) = (-1)^n(n+1)^{n-1}\int_0^\infty du' e^{-(n+1)y\,\text{ch}\,u'} = (-1)^n(n+1)^{n-1} K_0[(n+1)y], \tag{A.6}$$

where K_0 is the standard modified Bessel function (Gradshteyn and Ryzhik, 1980). In particular

$$I_0(y) = K_0(y). \tag{A.7}$$

We finally get from Eqs. A.2–4

$$P_1(\infty, y) = 1 - \exp\left\{-2n_0\varepsilon e^{-y} \sum_{n\geq 0} a^n I_n(y)\right\}. \tag{A.8}$$

Hence, the asymptotic un-entanglement probability depends on the dimensionless parameters $2n_0\varepsilon$ ($\simeq 5.76$), ε/L ($\simeq 1.610^{-2}$) and, more crucially, on the Sherwood number y, which is now made explicit.

Small y behavior

For y small, we have for $n = 0$

$$I_0(y) \equiv K_0(y) \simeq -\ln y + \mathbb{O}(1),$$

whereas for $n \geq 1$, $I_n(0)$ is a finite number. Hence, from Eq. A.7 we get

$$\begin{aligned} P_1(\infty, y) &= 1 - \exp[2n_0\varepsilon \ln y + \mathbb{O}(1)] \\ &\simeq 1 - cy^{2n_0\varepsilon}, \end{aligned} \tag{A.9}$$

where c is some constant (still depending on ε/L). Because $2n_0\varepsilon \simeq 5.76$, $P_1(\infty, y)$ approaches smoothly the value 1 at low Sherwood number.

Large y behavior

For $n = 0$, one has for $y \to \infty$

$$I_0(y) \equiv K_0(y) = \sqrt{\frac{\pi}{2y}}\, e^{-y}(1 + \mathbb{O}(1/y)), \tag{A.10}$$

whereas for $n \geq 1$

$$I_n(y) \leq I_n(0)e^{-(n+1)y}. \tag{A.11}$$

The leading term in Eq. A.8 is thus simply given by the $n = 0$ contribution

$$P_1(\infty, y) \underset{y\to\infty}{\simeq} 2n_0\varepsilon e^{-2y}\sqrt{\frac{\pi}{2y}}, \tag{A.12}$$

showing that the probability of removing any entanglement at a finite time is *exponentially* decreasing with the Sherwood number y, thus with the segregation speed v.

The curve $P_1(\infty, y)$ as a function of y is displayed in Fig. 4, exhibiting the characteristic (half) bell shape expected from the above study.

It may be interesting to note that both the small and large behaviors of $P(\infty, y)$ are dominated by the $n = 0$, i.e., K_0 term in Eq. A.8. Furthermore, the other terms obey the inequality A.11, and the expansion parameter a is biologically small. Hence, a good approximation of the one-unentanglement large-time probability $P_1(\infty, y)$ is simply obtained by retaining only the $n = 0$ term in Eq. A.8, arriving at

$$P_1(\infty, y) \simeq 1 - \exp[-2n_0\varepsilon e^{-y}K_0(y)], \tag{A.13}$$

which corresponds exactly to the simple approximation $\hat{P}_1(\infty, y)$ (Eq. 16).

APPENDIX B

Large α behavior of $P(\beta y, y)|_{y=0}$

It is interesting to study for completeness the value at zero Sherwood number $y = 0$ of the efficiency probability $P(\beta y, y)$. Starting from Eqs. 9 and 10 and performing the change of variable $\theta = y^2\theta'$ in Eq. 10:

$$\mathcal{P}[u, x, y] = \frac{\varepsilon}{2L}\frac{1}{\sqrt{\pi}}\, e^{-y}\int_0^{x/y^2} \frac{d\theta'}{\theta'^{3/2}} \exp\left[-y^2\theta' - \frac{1}{4\theta'}(1 + u^2)\right].$$

For $x = \beta y$ (actually, for $x = \beta y^\gamma$, $\gamma < 2$), we can now take the limit $y \to 0$, to get

$$\begin{aligned} \mathcal{P}[u, \beta y, y]_{y\to 0} &= \frac{\varepsilon}{2L}\frac{1}{\sqrt{\pi}}\int_0^\infty \frac{d\theta'}{\theta'^{3/2}} \exp\left[-\frac{1}{4\theta'}(1 + u^2)\right] \\ &= \frac{\varepsilon}{L}(1 + u^2)^{-1/2}. \end{aligned} \tag{B.1}$$

This gives for the probability (9)

$$\begin{aligned} &\mathcal{P}(x = \beta y, y)|_{y=0} \\ &\quad = 1 - \exp\left\{2n_0L\int_0^\alpha du \ln\left(1 - \frac{\varepsilon}{L}\frac{1}{\sqrt{1 + u^2}}\right)\right\}. \end{aligned} \tag{B.2}$$

At this stage, it is already clear that for α large, the first term for the expansion of the natural log function will yield a leading logarithmic singularity

$$\begin{aligned} \int_0^\alpha du\left(-\frac{\varepsilon}{L}\right)\frac{1}{(1 + u^2)^{1/2}} &= -\frac{\varepsilon}{L}\ln[\alpha + \sqrt{1 + \alpha^2}] \\ &= -\frac{\varepsilon}{L}\ln 2\alpha + \mathbb{O}(\alpha^{-2}). \end{aligned} \tag{B.3}$$

Neglecting as usual terms of relative order $\mathbb{O}[(\varepsilon/L)^2]$ in Eq. B.2, we therefore arrive at the asymptotic result

$$\begin{aligned} \mathcal{P}[\beta y, y, \alpha]_{y=0} &\underset{\alpha\to\infty}{=} 1 - \exp[-2n_0\varepsilon \ln 2\alpha + \mathbb{O}(\alpha^{-2})] \\ &= 1 - (2\alpha)^{-2n_0\varepsilon}(1 + \mathbb{O}(\alpha^{-2})). \end{aligned} \tag{B.4}$$

Notice that the same result can be derived from the approximate expression $\tilde{P}$ (14).

Therefore, for zero Sherwood number $y = 0$, the efficiency function $\mathcal{P}(\beta y, y)|_{y=0}$ reaches algebraically fast for α large its upper value 1 with an exponent $2n_0\varepsilon \simeq 5$–6.

This completes the very similar result obtained in Appendix A for $P(x = \infty, y, \alpha)$ in the reverse double limit $\alpha \to \infty$ and then $y \to 0$ (Eq. A.9):

$$P(x = \infty, y, \alpha = \infty) \underset{y\to 0}{\simeq} 1 - cy^{2n_0\varepsilon}.$$

We thank Cyprien Gay, David Kosower, and Carl Mann for fruitful discussions, and Claudine Verneyre for numerical assistance.

REFERENCES

Albery, W. J., and J. R. Knowles. 1976. Evolution of enzyme function and the development of catalytic efficiency. *Biochemistry.* 15:5631–5640.

Alexander, S. P., and C. L. Rieder. 1991. Chromosome motion during attachment to the vertebrate spindle: initial saltatory-like behavior of chromosomes and quantitative analyses of force production by nascent kinetochore fibers. *J. Cell. Biol.* 113:805–815.

Bajer, A. 1963. Observations of dicentrics in living cells. *Chromosoma.* 14:18–30.

Bajer, A. S., and J. Molé-Bajer. 1972. Spindle dynamics and chromosome movements. *Int. Rev. Cytol. Suppl.* 3(Suppl.):1–271.

Bennett, S. P., and S. E. Halford. 1989. Recognition of DNA by type II restriction enzymes. *Curr. Top. Cell. Regul.* 30:57–104.

Downes, C. S., A. M. Mullinger, and R. T. Johnson. 1991. Inhibitors of DNA topoisomerase II prevent chromatid separation in mammalian cells but do not prevent exit from mitosis. *Proc. Natl. Acad. Sci. USA.* 88:8895–8899.

Drake, F. H., G. A. Hofmann, H. F. Bartus, M. R. Mattern, S. T. Crooke, and C. K. Mirabelli. 1989. Biochemical and pharmacological properties of p170 and p180 forms of topoisomerase II. *Biochemistry.* 28: 8154–8160.

Fersht, A. 1985. Enzyme Structure and Mechanism. Freeman, New York.

Gasser, S. M., T. Laroche, J. Falquet, E. Boy de la Tour, and U. K. Laemmli. 1986. Metaphase chromosome structure. Involvement of topoisomerase II. *J. Mol. Biol.* 188:613–629.

Gradshteyn, I. S., and I. M. Ryzhik. 1980. Tables of Integrals, Series, and Products. Academic, London.

Holm, C. 1994. Coming undone: how to untangle a chromosome. *Cell.* 77:955–957.

Holm, C., T. Goto, J. C. Wang, and D. Botstein. 1985. DNA topoisomerase II is required at the time of mitosis in yeast. *Cell.* 41:553–563.

Holm, C., T. Stearns, and D. Botstein. 1989. DNA topoisomerase II must act at mitosis to prevent nondisjunction and chromosome breakage. *Mol. Cell. Biol.* 9:159–168.

Hyrien, O., and M. Méchali. 1993. Chromosomal replication initiates and terminates at random sequences but at regular intervals in the ribosomal DNA of *Xenopus* early embryos. *EMBO J.* 12:4511–4520.

Krueger, S., G. Zaccai, A. Wlodawer, J. Langowski, M. O'Dea, A. Maxwell, and M. Gellert. 1990. Neutron and light-scattering studies of DNA gyrase and its complex with DNA. *J. Mol. Biol.* 211:211–220.

Le Gall, J.-F. 1986. Sur la saucisse de Wiener et les points multiples du mouvement Brownien. *Ann. Prob.* 14:1219–1244.

Lindsley, J.E., and J.C. Wang. 1993. On the coupling between ATP usage and DNA transport by yeast DNA topoisomerase II. *J. Biol. Chem.* 268:8096–8104.

Mazia, D. 1961. Mitosis and the physiology of cell division. *In* The Cell. J. Brachet and A. E. Mirsky, editors. Academic Press, New York. 77–412.

McDowall, A. W., J. M. Smith, and J. Dubochet. 1986. Cryo-electron microscopy of vitrified chromosomes in situ. *EMBO J.* 5:1395–1402.

Nicklas, R. B. 1988. The forces that move chromosomes in mitosis. *Annu. Rev. Biophys. Biophys. Chem.* 17:431–449.

Osheroff, N., E. R. Shelton, and D. L. Brutlag. 1983. DNA topoisomerase II from *Drosophila melanogaster*. Relaxation of supercoiled DNA. *J. Biol. Chem.* 258:9536–9543.

Permana, P. A., C. A. Ferrer, and R. M. Snapka. 1994. Inverse relationship between catenation and superhelicity in newly replicated simian virus 40 daughter chromosomes. *Biochem. Biophys. Res. Commun.* 201: 1510–1517.

Pienta, K. J., and D. S. Coffey. 1984. A structural analysis of the role of the nuclear matrix and DNA loops in the organization of the nucleus and chromosome. *J. Cell. Sci. Suppl.* 1:123–135.

Purcell, E. M. 1977. Life at low Reynolds number. *Am. J. Phys.* 45:3–11.

Rattner, J. B., and C. C. Lin. 1985. Radial loops and helical coils coexist in metaphase chromosomes. *Cell.* 42:291–296.

Saitoh, Y., and U. K. Laemmli. 1994. Metaphase chromosome structure: bands arise from a differential folding path of the highly AT-rich scaffold. *Cell.* 76:609–622.

Schomburg, U., and F. Grosse. 1986. Purification and characterization of DNA topoisomerase II from calf thymus associated with polypeptides of 175 and 150 kDA. *Eur. J. Biochem.* 160:451–457.

Shamu, C. E., and A. W. Murray. 1992. Sister chromatid separation in frog egg extracts requires DNA topoisomerase II activity during anaphase. *J. Cell. Biol.* 117:921–934.

Sparrow, A. H., C. L. Huskins, and G. B. Wilson. 1941. Studies on the chromosome spiralization cycle in *Trillium. Can. J. Res. Sec. C.* 19: 323–350.

Spell, R. M., and C. Holm. 1994. Nature and distribution of chromosomal intertwinings in *Saccharomyces cerevisiae. Mol. Cell. Biol.* 14: 1465–1476.

Sundin, O., and A. Varshavsky. 1981. Arrest of segregation leads to accumulation of highly intertwined catenated dimers: dissection of the final stages of SV40 DNA replication. *Cell.* 25:659–669.

Swedlow, J. R., J. W. Sedat, and D. A. Agard. 1993. Multiple chromosomal populations of topoisomerase II detected in vivo by time-lapse, three-dimensional wide-field microscopy. *Cell.* 73:97–108.

Taylor, E. W. 1965. Brownian and saltatory movements of cytoplasmic granules and the movement of anaphase chromosomes. *In* Proceedings of the Fourth International Congress on Rheology. Part 4. Symposium on Biorheology A. L. Copley, editor. Interscience, New York. 175–191.

Wang, J. C. 1991. DNA topoisomerases: why so many? *J. Biol. Chem.* 266:6659–6662.

Wasserman, S. A., J. H. White, and N. R. Cozzarelli. 1988. The helical repeat of double-stranded DNA varies as a function of catenation and supercoiling. *Nature.* 334:448–450.

Watt, P. M., E. J. Louis, R. H. Borts, and I. D. Hickson. 1995. Sgs 1: a eukaryotic homolog of E. coli RecQ that interacts with topoisomerases II in vivo and is required for faithful chromosome segregation. *Cell.* 81:253–260.

Zechiedrich, E. L., and N. Osheroff. 1990. Eukaryotic topoisomerases recognize nucleic acid topology by preferentially interacting with DNA cross-overs. *EMBO J.* 9:4555–4562.

Zhu, J. G., C. S. Newlon, and J. A. Huberman. 1992. Localization of a DNA replication origin and termination zone on chromosome III of *Saccharomyces cerevisiae. Mol. Cell. Biol.* 12:4733–4741.

Zimmermann, S. B., and A. P. Minton. 1993. Macromolecular crowding: biochemical, biophysical, and physiological consequences. *Annu. Rev. Biophys. Biomol. Struct.* 22:27–65.